

Carbonic Anhydrase-Embedded ZIF-8 Electrospun PVA Fibers as an Excellent Biocatalyst Candidate

Vahideh Asadi, Afsaneh Marandi, Reihaneh Kardanpour, Shahram Tangestaninejad,*
Majid Moghadam,* Valiollah Mirkhani,* Iraj Mohammadpoor-Baltork, and Razieh Mirzaei



Cite This: *ACS Omega* 2023, 8, 17809–17818



Read Online

ACCESS |



Metrics & More

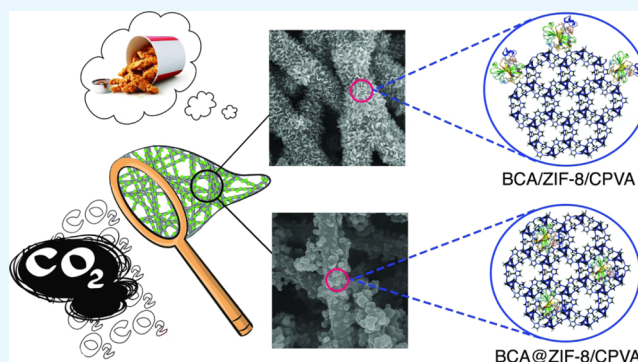


Article Recommendations



Supporting Information

ABSTRACT: There is a growing concern that the increasing concentration of CO₂ in the atmosphere contributes to a potential negative impact on global climate change. To deal with this problem, developing a set of innovative, practical technologies is essential. In the present study, maximizing the CO₂ utilization and precipitation as CaCO₃ was evaluated. In this manner, bovine carbonic anhydrase (BCA) was embedded into the microporous zeolite imidazolate framework, ZIF-8, *via* physical absorption and encapsulation. Running as crystal seeds, these nanocomposites (enzyme-embedded MOFs) were *in situ* grown on the cross-linked electrospun polyvinyl alcohol (CPVA). The prepared composites displayed much higher stability against denaturants, high temperatures, and acidic media than free BCA, and BCA immobilized into or on ZIF-8. During 37 days of storage period study, BCA@ZIF-8/CPVA and BCA/ZIF-8/CPVA maintained more than 99 and 75% of their initial activity, respectively. The composition of BCA@ZIF-8 and BCA/ZIF-8 with CPVA improved stability for consecutive usage in recovery reactions, recycling easiness, and greater control over the catalytic process. The amounts of calcium carbonate obtained by one mg each of fresh BCA@ZIF-8/CPVA and BCA/ZIF-8/CPVA were 55.45 and 49.15 mg, respectively. The precipitated calcium carbonate by BCA@ZIF-8/CPVA reached 64.8% of the initial run, while this amount was 43.6% for BCA/ZIF-8/CPVA after eight cycles. These results indicated that the BCA@ZIF-8/CPVA and BCA/ZIF-8/CPVA fibers could be efficiently applied to CO₂ sequestration.



1. INTRODUCTION

The climate change and CO₂ pollution threaten public health globally.^{1,2} With the carbon cycle's excess emission, several strategies, including capture and storage or converting CO₂ into fuels and chemicals, have been proposed to solve the environmental problem.³ As far as CO₂ transformation is concerned, the main methods, which can be used to deal with this issue, are chemical, physical, and enzymatic reactions. Enzymatic reactions are considered a promising approach because they are environmentally friendly.^{4,5} However, a significant limitation of free enzymes is that their instability restricts their potential for widespread industrial applications.⁶ Immobilization technology is a desirable method used for enhancing the industrialization of enzymes as biocatalysts as well as improving their catalytic properties such as stability, activity, and tolerance to denaturants.^{7–9} In this sense, two crucial points need to be considered: selecting a suitable support and the immobilization method.¹⁰

Currently, the commonly used supports for enzyme immobilization are natural polymers, carbon nanotubes, graphene oxide, and so on.^{11–13} These materials can effectively improve the activity and stability of enzymes and reduce the

inhibition of products. Despite these excellent properties, the current applications of the immobilized enzymes with these materials are still limited due to low loading efficiency, inflexible pore sizes, and so on. Therefore, it is a great necessity to explore novel immobilization matrices. During the last few decades, the development of porous nanomaterials has made remarkable achievements.^{14,15} In particular, metal–organic frameworks (MOFs) and covalent organic frameworks, as novel porous framework materials, have been widely used in various fields.¹⁶ Compared with other supports for enzyme immobilization, these materials have better biocompatibility, tuneability, and crystallinity. MOFs are a kind of porous crystal organic–inorganic hybrid materials formed by metal nodes and organic ligands.¹⁷

Received: February 2, 2023

Accepted: April 27, 2023

Published: May 9, 2023



The second decisive factor in enzyme performance is the selected immobilization method, which affects enzyme activity and reusability. Physical adsorption is one of the simple and common methods of immobilization in which hydrogen bonding forces, van der Waals forces, or hydrophobic interactions play roles in enzyme adsorption on the support.⁸ The strengths of this method are simplicity, cost-effectiveness, and independency of the chemical reaction. Since the adsorption process is reversible and based on weak forces, the possibility of enzyme detachment from the support is high.¹⁸ In the encapsulation method, the enzyme species are entrapped in the support network without attachment. In this method, the integration of MOF synthesis and enzyme addition occurs in one pot rather than the injection of enzymes into a pre-synthesized structure, called *de novo* encapsulation. A favorable 3D microenvironment for enzymes is provided that prevents enzymes from denaturation and deactivation. In addition, the enzyme leaching is negligible due to the framework of MOFs surrounding enzymes.¹⁶ It is worth emphasizing that this strategy usually needs to be implemented under mild conditions (e.g., aqueous solution and room temperature) to prevent enzymes from denaturation, which overcome the restrictions of water stability issue caused by most MOFs prepared in organic solvents. Zeolitic imidazolate framework-8 (ZIF-8) is the most commonly used skeleton due to its mild synthesis conditions and almost negligible toxicity.¹⁹

Carbonic anhydrase (CA, EC 4.2.1.1) is considered a zinc metalloenzyme that has been widely accepted for its reversible catalysis of the sequestration of CO₂ to bicarbonate, which occurs at a slow pace in the absence of a catalyst.²⁰ The lack of reusability and sensitivity in harsh conditions restricts the performance of free enzymes for CO₂ capture in the industrial processes.²¹ In recent years, CA has been immobilized successfully on/into various support materials, such as nanoparticles, nanofibers, hollow nanofibers, biopolymers, membranes, and microspheres.^{9,22–26}

ZIF-8 has mainly been taken into practice as immobilization support because of its high thermal and chemical stability, vital permanent porosity, and ability to grow under mild conditions, which are crucial for the preservation of the enzyme.²⁷ Up to now, CA has been immobilized either by *de novo* encapsulation²⁸ or adsorption.^{29,30} Recently, the bovine CA (BCA) has been successfully immobilized into the crystalline hybrid framework of ZIF-8 in our research group *via* the *de novo* approach.³¹ This biocatalyst displayed superior CO₂ capture capacity compared to the free BCA. Despite being demonstrated to have an adsorption capacity for CO₂, the recyclability and mechanical strength of ZIF-8 still need to be improved for industrial applications. Moreover, ZIF-8 can be easily destroyed under acidic conditions, which limits its practical applications. To overcome this drawback, Cui *et al.* applied a silica layer around the enzyme/ZIF-8 particles to provide a shield to protect the enzyme from chemical degradation.³² Furthermore, enzymes@ZIF-8 composites have been protected with nanocoating and mesoporous silica shells.^{33,34}

Over the last few years, biopolymers have been considered an alternative membrane material for immobilizing enzymes.^{35,36} So far, many polymer–MOF composites have been reported in various forms, such as binders or films;^{37–40} however, fibrous substrates are the best candidates for MOF particles. The hierarchical porous structure of MOF–polymer fibers combines the preponderances of both sets of materials.

The three-dimensional network of fibers can prevent aggregation and improve the dispersion of MOF particles, consequently improving the regeneration and control of the composites. The electrospinning technique is a highly versatile and simple method used to consistently produce polymeric nano-/microfibers with desirable properties.⁴¹ Among various types of biopolymers, poly(vinyl alcohol) has captured so much attention because of its distinct properties, such as high thermal, chemical, and mechanical stability. Due to the solubility of poly(vinyl alcohol) in water media, it was cross-linked after electrospinning *via* the glutaraldehyde treatment to be hydrophobic during the enzyme immobilization in aqueous media.⁴²

In the present study, BCA molecules were embedded into ZIF-8 *via* physical adsorption and encapsulation. Running as crystal seeds, these nanocomposites (enzyme-embedded MOFs) were *in situ* grown on the electrospun polyvinyl alcohol fibers. Anchoring of enzyme-embedded MOFs on the surface of the electrospun polyvinyl alcohol fibers increases the enzyme's stability, prevents its leaching, and guides the scientists to use fibrous composites with simple separation and excellent reusability.⁴³ Notably, the biocatalytic composites showed an excellent CO₂ capture capacity compared to the conventional BCA@ZIF-8 and free BCA.

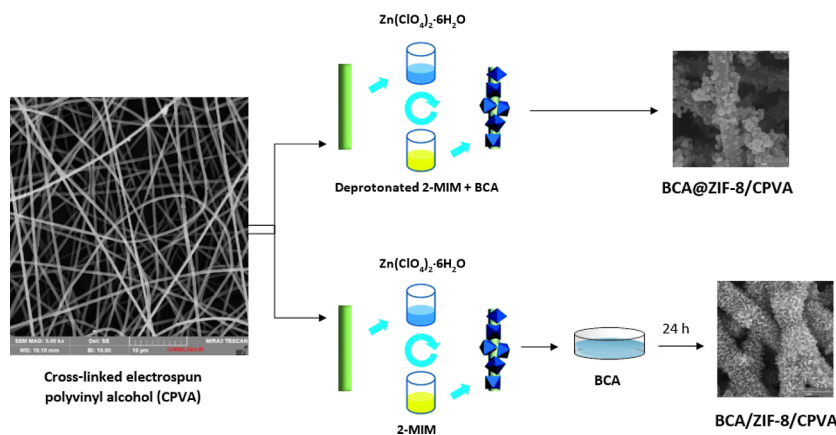
2. MATERIALS AND METHODS

2.1. Materials. Materials used in this research study such as BCA (lyophilized powder), 2-methylimidazole (2-mim, 98%), zinc perchlorate hexahydrate [Zn(ClO₄)₂·6H₂O], triethylamine (TEA), 2-amino-2-(hydroxymethyl)-1,3-propanediol (Tris base), *p*-nitrophenol, *p*-nitrophenyl acetate (*p*-NPA), anhydrous calcium chloride (CaCl₂), and protein assay reagents (specifically used for producing the Bradford reagent) were all purchased from Aldrich and used without purification, PVA (*M_w* ~ 72 000, hydrolysis degree 99.8%) was purchased from AppliChem, and the rest of the reagents were purchased from Merck or Fluka as ACS reagent-grade chemicals. All solutions were prepared with deionized (DI) water.

2.2. Characterization. X-ray diffraction (XRD) patterns of the samples were recorded on a Bruker D8-Advance diffractometer using a Cu K α anode ($\lambda = 1.7890 \text{ \AA}$) in the range 0.5 to 70°. Fourier transform infrared (FT-IR) spectroscopy was recorded in the range of 4000–400 cm⁻¹ on a JASCO FT-IR 6300 spectrometer. Field emission scanning electron microscopy (FE-SEM) images and dispersive energy analysis of X-ray were performed on a MIRA3 instrument from TESCAN, and thermogravimetric analyses (TGA) were performed on a PerkinElmer STA 6000 thermal analyzer. The surface properties of nanocomposites were calculated by adsorption–desorption of N₂ gas at 77 K using a BELSORP mini II instrument after pretreatment. The UV–vis spectra were recorded on a JASCO V-570 spectrophotometer. Preparation of the fibers was performed using an electrospinning instrument made by Fanavaran Nano Meghyas Co., Iran. The synthesis procedure of electrospinning solutions, electrospun fibers, and cross-linked PVA are presented in the [Supporting Information](#).

2.3. Preparation of Cross-Linked PVA. Glutaraldehyde (GA) in acetone solution was used as the crosslinking agent according to a formerly reported method by Kim *et al.*⁴² In this procedure, the synthesized electrospun PVA was mixed with GA (0.03 M) and HCl (0.01 M) in an acetone solution and kept for 24 h without stirring. The cross-linked nanofibers were

Scheme 1. Preparation of BCA@ZIF-8/CPVA and BCA/ZIF-8/CPVA Composites



washed with acetone and sequentially with DI water to remove traces of the GA and HCl. They were soaked in DI water until used.

2.4. Preparation of BCA@ZIF-8/CPVA. In a typical experiment, cross-linked PVA was immersed in a mixture containing 5 mL of 2-methylimidazole (0.16 mg mL^{-1} deprotonated with 0.3 mL TEA) and BCA solution (10 mg mL^{-1} in 50 mM Tris buffer, pH 8.0) for 5 min. Then it was immersed in an aqueous solution of $\text{ZnClO}_4 \cdot 6\text{H}_2\text{O}$ (126.6 mg mL^{-1}) for 5 min, taken out, followed by washing with Tris buffer and DI water. This cycle was repeated several times to achieve the maximum loading of BCA@ZIF-8 on the CPVA. The resulting cross-linked BCA@ZIF-8/CPVA composite was washed with Tris buffer and DI water, followed by drying at 25°C . The amount of BCA in the enzyme solution before and after immobilization was determined using the Bradford method (Figure S1, Supporting Information).⁴⁴ As a control, the ZIF-8/CPVA composite was synthesized in the absence of the BCA enzyme with the same method.

2.5. Preparation of BCA/ZIF-8/CPVA. In order to synthesize the BCA/ZIF-8/CPVA composite, two solutions were prepared: solution A, 2-methylimidazole (1.08 g) in DI water (4.5 mL), and solution B, $\text{ZnClO}_4 \cdot 6\text{H}_2\text{O}$ (0.1383 g) in DI water (4 mL). Cross-linked PVA was immersed in solution A for 5 min and washed with Tris buffer and DI water consequently. Then it was immersed in solution B for 5 min, taken out, and washed again. This cycle was repeated several times, and the resulting ZIF-8/CPVA composite was immersed in a BCA solution (2 mg in 50 mM Tris buffer, pH 8.0) for 24 h, washed with Tris buffer and DI water, and dried at 25°C . The amount of BCA in the enzyme solution before and after immobilization was determined using the Bradford method.

Scheme 1 illustrates the preparation procedure of BCA@ZIF-8/CPVA via encapsulation and BCA/ZIF-8/CPVA via physical adsorption.

2.6. Encapsulation and Activity Detection. The enzyme activity of the free and immobilized BCA, which was enhanced by *p*-NPA hydrolysis at room temperature, was measured by monitoring the increase in the absorption band at 405 nm. The assay mixture consisted of 2.7 mL of Tris buffer (50 mM, pH 8.0), 0.3 mL of substrate solution (0.5, 1, 1.5, 2, 2.5 mM *p*-NPA dissolved in acetonitrile), and 3 mg of immobilized BCA; the latter being mixed in a 3 mL cuvette using a micropipette. The enzyme activity was measured with a UV–vis spectrophotometer. Blank experiments were also conducted in the absence of the catalyst to estimate the self-dissociation of

p-NPA in each assay solution. The activity of free enzyme was equaled to 1 in this study, and the relative activity of composites was calculated using it.

2.7. Effect of pH. To investigate the optimum pH value, the prepared composites were incubated in Tris buffer solution (50 mM) in the pH range of 6–10 at RT. After 1 h, the residual activities of the free and encapsulated enzyme were determined as described above.

2.8. Thermal Stability. The thermal stability of the prepared composites was determined by incubating them into 50 mM Tris buffer at pH = 8 in the temperature range of 30–70 $^\circ\text{C}$ for 1 h. Afterward, the relative activities were calculated as mentioned above.

2.9. Storage Stability. The immobilized enzyme was stored for 37 days at room temperature to determine whether the immobilization provided a suitable environment for its storage stability in Tris buffer (50 mM, pH 8.0).

2.10. Activity Recovery. In order to investigate the reusability of the immobilized BCA, the performance of the synthesized composites was evaluated by *p*-NPA hydrolysis. In this way, after each run, the composite was separated and washed thoroughly with Tris buffer and reused for the next run. The enzyme activity of the immobilized BCA was measured as described in the Encapsulation and Activity Detection section.

2.11. CO₂ Sequestration in CaCO₃. Generally, hydration of CO₂ and its subsequent sequestration as CaCO₃ in the presence of free and immobilized BCA were performed as follows: initially, CO₂ gas was introduced into 20 mL of DI water at a constant flow rate for 30 min. Then, 2 mg of free BCA was added to a 10 mL Tris buffer solution (pH = 8.0) at the fixed optimum temperature of 25°C . The enzyme-containing solution was added to the CO₂ solution, and the mixture was continuously stirred for about 30 min. The hydrated CO₂ solution was filtered, and subsequently, 0.9 g CaCl₂·2H₂O was added to the filtrate. The resulting CaCO₃ was filtered and weighed after drying. Finally, the above procedure was applied to the equivalent amount of enzyme in composites.

2.12. Recovery and Reuse of the Biocatalyst. The reusability of the prepared composite was evaluated in sequential CO₂ sequestration. In this manner, after accomplishing each cycle, the prepared biocatalyst was withdrawn, washed with Tris buffer, and immersed in a fresh reaction mixture to carry out the next cycle.

3. RESULTS AND DISCUSSION

3.1. Preparation and Characterization of the Biocatalyst. It is widely known that CA is considered the fastest enzyme for catalyzing the conversion of one million CO₂ molecules to bicarbonate per second.⁴⁵ In this spot, we introduced the BCA enzyme molecules in the ZIF-8. Regarding the combination of enzyme and ZIF-8, the enzyme activity was significantly improved after immobilization in ZIF-8. To enhance the separation performance for large-scale industrial processes, a strategy was taken to fabricate the biocatalytic composites of BCA@ZIF-8. Particularly, the BCA was embedded in the insight pore aperture of ZIF-8 with good biocompatibility. In this situation, a protective shell was formed by ZIF-8 around the immobilized BCA. The mixtures of cross-linked polyvinyl alcohol (CPVA) fibers and BCA were added into the precursor of the ZIF-8 solution. BCA@ZIF-8 seeds were prepared, and the CPVA fibers provide a setting for the homogeneous dispersion of them. In the second part of this work, CPVA fibers were immersed into the precursor of ZIF-8 solution, and then the BCA enzyme was added through physical absorption. To characterize these materials, a series of tests were conducted. As shown in Figure 1, the powder XRD

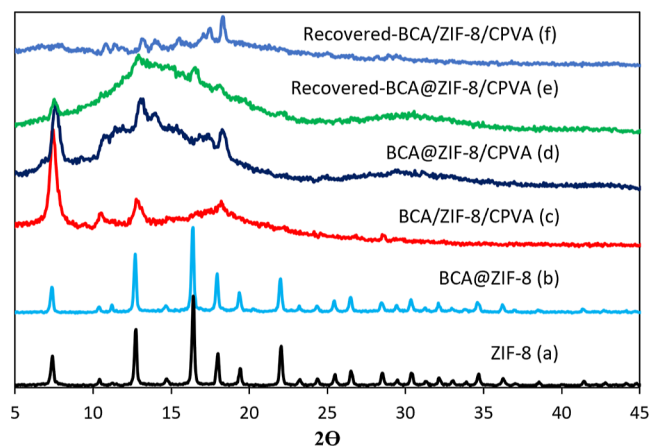


Figure 1. XRD patterns of ZIF-8 (a), BCA@ZIF-8 (b), BCA/ZIF-8/CPVA (c), BCA@ZIF-8/CPVA composite (d), recovered BCA/ZIF-8/CPVA (e), and recovered BCA@ZIF-8/CPVA (f).

pattern of ZIF-8 and the prepared composites match well with the literature. CPVA nanofiber is an amorphous polymer. The additional peaks in the synthesized composites agreed well with the patterns of the pure ZIF-8 (Figure 1),⁴⁶ clearly indicating that the incorporation of the enzyme did not affect the crystal structure of ZIF-8.

The FT-IR spectra of samples are shown in Figure 2. In the reflectance FT-IR spectra of cross-linked PVA nanofibers, the most influential band between 3040 and 3673 cm⁻¹ belongs to the O–H functional groups, and the band appeared at 1700 cm⁻¹ belongs to the acetate groups (Figure 2a). The vibrational bands in the range of 600–1500 cm⁻¹ correspond to the characteristic stretching and bending modes of the imidazole ring (Figure 2b).⁴⁷ Also, the band at 1580 cm⁻¹ is ascribed to the stretching mode of C=N in 2-mim, whereas the bands at 2927 and 3131 cm⁻¹ can be related to the stretching mode of C–H of the aromatic ring and the aliphatic chain of 2-mim, respectively.

Also, the band at 420 cm⁻¹ represents the Zn–N stretching, which corresponds to the bonding between the Zn²⁺ cations

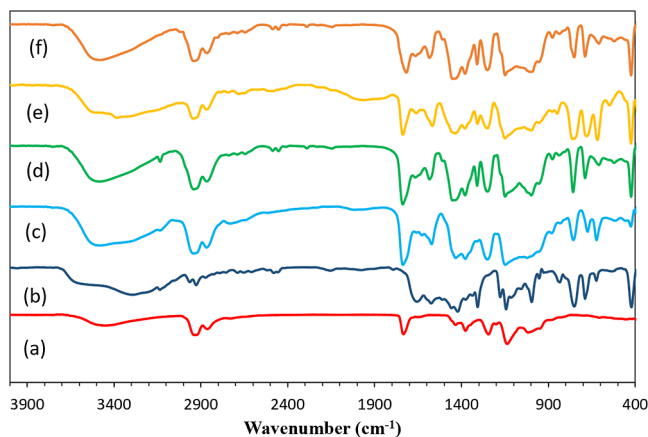


Figure 2. FT-IR spectra of CPVA fibers (a), BCA@ZIF-8 (b), BCA/ZIF-8/CPVA (c), BCA@ZIF-8/CPVA composite (d), recovered BCA/ZIF-8/CPVA (e), and recovered BCA@ZIF-8/CPVA (f).

and 2-mim to form imidazolate.⁴⁸ As shown in Figure 2c,d, all previous bands are well maintained in the biocatalyst spectrum. Additionally, the existence of the band at 1648 cm⁻¹ corresponding to double bonds and C=O stretching modes of the enzyme verified the presence of the protein in the composites.⁴⁹ Moreover, the free BCA spectrum exhibited stretching bands at 1500–1550 cm⁻¹ corresponding to amide II bonds and NH stretching vibration, which was visible in the biocatalyst spectrum, confirming the presence of the BCA within the composites.

The UV–vis spectra of the synthesized fibers provide another indication of the presence of BCA in the fibers. As seen in Figure 3, in addition to the absorption bands

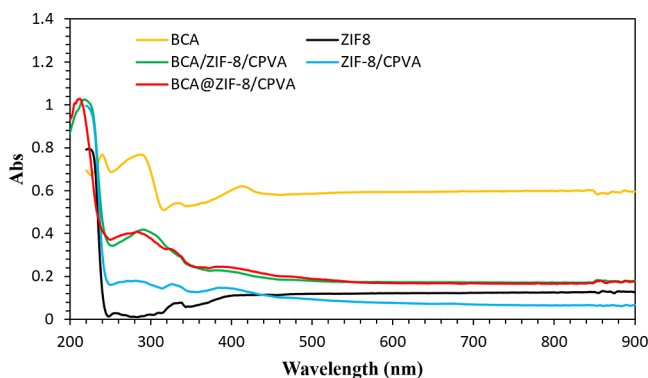


Figure 3. UV–vis spectra of BCA, ZIF-8, ZIF-8/CPVA, BCA/ZIF-8/CPVA, and BCA@ZIF-8/CPVA composites.

corresponding to the ZIF-8 and CPVA, an extra absorption band around 286 and 293 nm was attributed to the BCA embedded on or into the framework.⁵⁰ It should be noted that an adsorption band at 223 nm in ZIF-8 spectra attributed to the $\pi \rightarrow \pi^*$ and $n \rightarrow \pi^*$ transitions of 2-methylimidazole that due to interaction with enzyme shift to 211 and 217 nm in BCA@ZIF-8/CPVA and BCA/ZIF-8/CPVA, respectively.

To examine the surface morphology of the synthesized composites, the samples were characterized using FE-SEM (Figure 4). It can be retrieved from Figure 4 that cubic ZIF-8 nanoparticles are clearly visible on the CPVA surface (Figure 4a,c,e), and the morphology of ZIF-8 did not affect during immobilization of the enzyme and fabrication of the CPVA

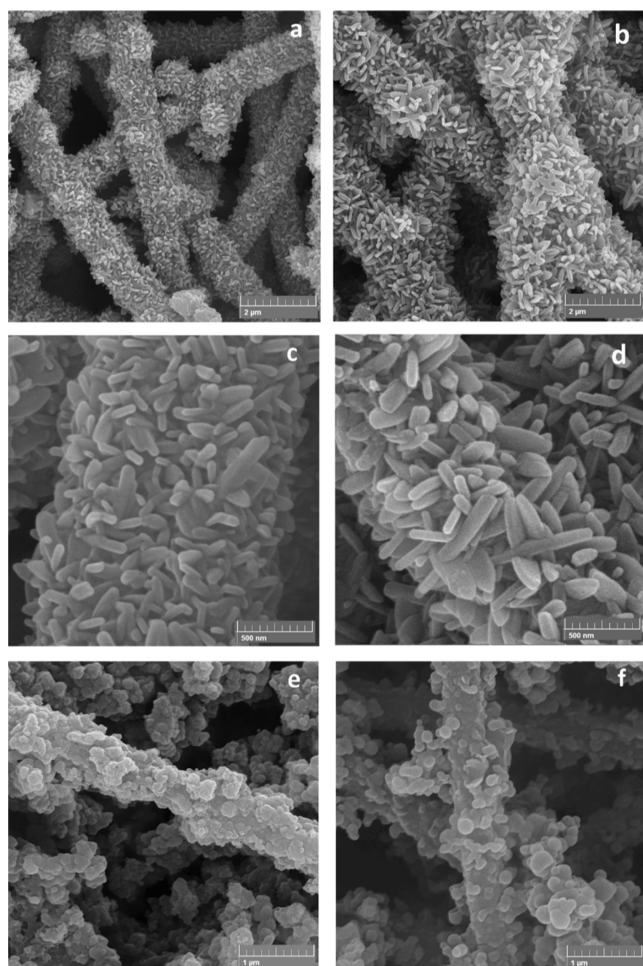


Figure 4. FE-SEM images of ZIF-8/CPVA (a,c,e), BCA/ZIF-8/CPVA (b,d), and BCA@ZIF-8/CPVA (f) composites.

surface (Figure 4b,d,f). In the case of the BCA/ZIF-8/CPVA composite, the ZIF-8 structure looks like fried chicken due to immersion in BCA solution for 24 h (Figure 4b,d).

The effective surfaces and porosity of the ZIF-8 and the biocatalysts were determined using N_2 physisorption measurements at 77 K (Figures 5 and S2). The results summarized in Table 1 indicate a noticeable decrease in Brunauer–Emmett–

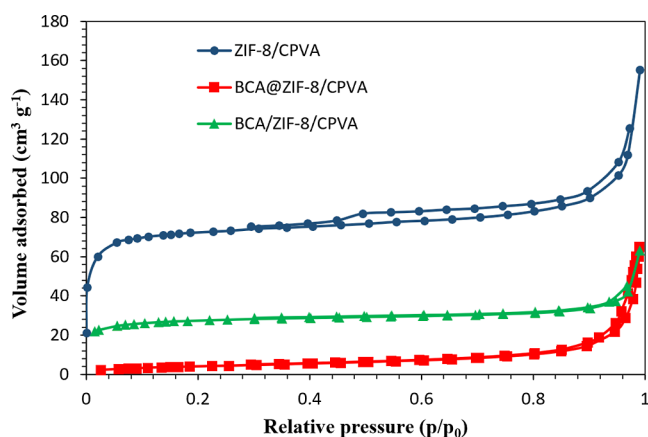


Figure 5. N_2 adsorption isotherms of ZIF-8/CPVA, BCA/ZIF-8/CPVA, and BCA@ZIF-8/CPVA composites at 77 K.

Table 1. BET Results of the ZIF-8 and Obtained Composites

samples	S_{BET} ($\text{m}^2 \text{g}^{-1}$)	total pore volume ($\text{cm}^3 \text{g}^{-1}$)	total pore diameter (nm)
ZIF-8/CPVA	290	0.24	3.3
BCA@ZIF-8/CPVA	15	0.1	6.1
BCA/ZIF-8/CPVA	105	0.1	3.7

Teller (BET) surface area of ZIF-8/CPVA (parent ZIF-8 embedded on CPVA) after encapsulation of BCA from 290 to $15 \text{ m}^2 \text{g}^{-1}$ for BCA@ZIF-8/CPVA. This is in total agreement with the occupation of the pores of the parent framework by enzyme groups. Furthermore, the average pore diameter of ZIF-8 increased from 3.3 to 6.1 nm after encapsulation in the BCA@ZIF-8/CPVA composite, indicating an increase in the pore size associated with the diameter of the encapsulated enzyme. In addition, in the case of enzyme surface adsorption for BCA/ZIF-8/CPVA, the surface area of $105 \text{ m}^2 \text{g}^{-1}$ was observed, and there is no meaningful change in the average pore diameter for this composite.

The TGA and DTG curves provide some data on the thermal stability of BCA/ZIF-8/CPVA and BCA@ZIF-8/CPVA (Figures 6 and S3). As it is shown in Figure 6, an initial

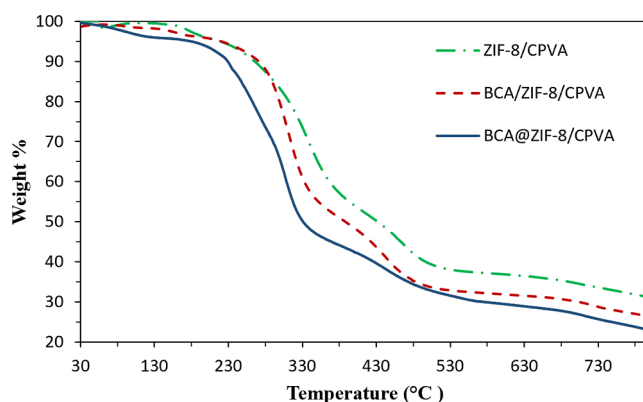


Figure 6. TGA curves of ZIF-8/CPVA, BCA/ZIF-8/CPVA, and BCA@ZIF-8/CPVA composites at 77 K.

weight loss was indicated *via* the TGA curve of both composites related to the removal of guest water molecules and residual imidazole and unreacted glutaraldehyde in the pores (about 10%), followed by the subsequent weight loss in the range of 200–380 °C attributed to the loss of the ZIF-8 framework and thermal decomposition of C–C bonds of PVA. The third peak at 380–530 °C is due to the decomposition of the main chains of PVA. In the case of BCA/ZIF-8/CPVA and BCA@ZIF-8/CPVA, the BCA enzyme loss occurs at the last two steps. Through comparing the TGA curves of BCA/ZIF-8/CPVA and BCA@ZIF-8/CPVA in steps 2 and 3, it can be retrieved that the weight loss of BCA@ZIF-8/CPVA and BCA/ZIF-8/CPVA is more significant than that of ZIF-8/CPVA, which proves the claim about the presence of BCA in the framework.^{49,51}

3.2. Biocatalyst Activity Evaluation. By considering the deactivation of the enzyme under reaction conditions, the catalytic activity of the prepared composites was first investigated as a function of pH, temperature, reusability, and storage. In this manner, the hydrolysis of *p*-NPA was followed spectrophotometrically by observing the formation of

Table 2. Kinetic Parameters, Relative Activity

samples	loaded enzyme ($\mu\text{g}/\text{mg}$ of support) ^a	K_m (mM)	K_{cat}/K_m ($\text{M}^{-1} \text{s}^{-1}$)	relative activity
BCA		8.92	399.80	1.00
BCA@ZIF-8/CPVA	69	5.14	499.75	1.25
BCA/ZIF-8/CPVA	63	7.25	443.78	1.11

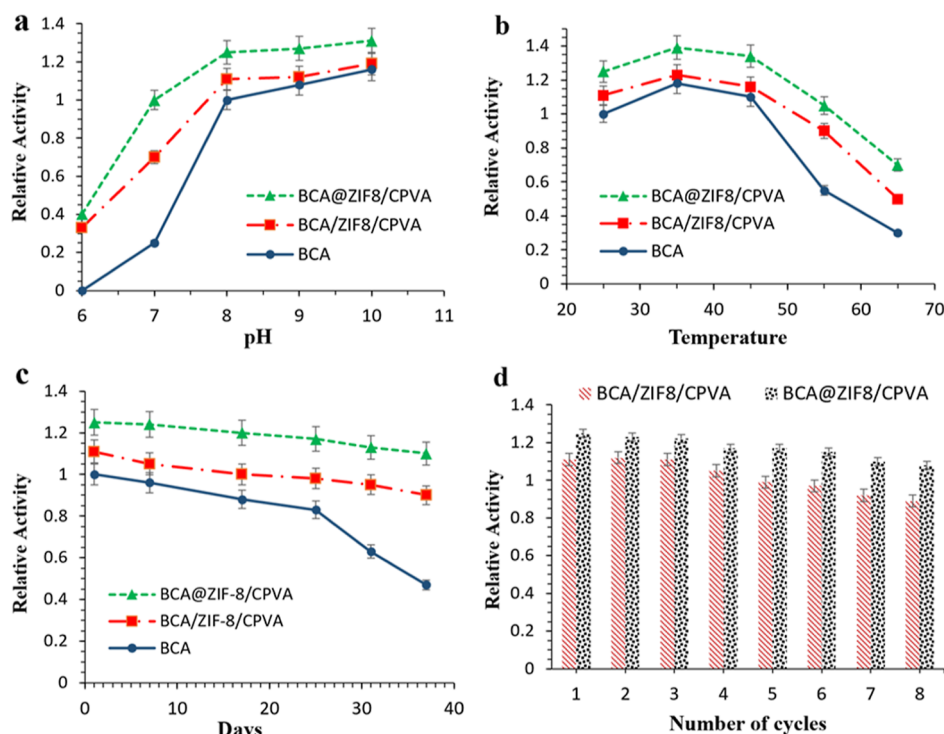
^aBy Bradford method.

Figure 7. (a) Effect of pH, (b) temperature, (c) storage stability, and (d) reusability of the biocatalysts [error bars are mean \pm standard deviation ($n = 3$)].

the *p*-nitrophenolate (*p*-NP) and acetic acid. Due to the similarity between esterase and CO_2 hydration reactions, the esterase activity of CA was measured to evaluate enzyme activity. This inexpensive method provides quick results that accurately detect changes in enzyme activity, environmental factors, and stability. By assessing the enzyme's catalytic process, we were able to study its potential for CO_2 sequestration. The optimum condition of $\text{pH} = 8$ at room temperature was selected based on the CO_2 hydration reaction equilibration. The obtained results were explained in detail in the following parts.

3.3. Kinetic Parameters. The kinetic parameters for the hydrolysis of *p*-NPA were estimated using the Michaelis–Menten and Lineweaver–Burk equations shown in eqs 2 and 3.

Based on the Michaelis–Menten kinetic model, a primary interaction between the substrate (*S*) and enzyme (*E*) leads to the formation of an enzyme–substrate (*ES*) complex intermediate. In the next step, while the product (*P*) forms, the enzyme regenerates in the reaction media (eq 1).



Both free and immobilized enzyme activities were determined at room temperature in 50 mM Tris buffer at $\text{pH} 8.0$. The graphs were plotted using different substrate concentrations and their corresponding reaction rates. The reciprocal of substrate concentration ($1/S$) was plotted against

the reciprocal of reaction rate ($1/V$) according to the following equations

$$V = \frac{K_{\text{cat}}[\text{S}][\text{E}_0]}{K_m + [\text{S}]} \quad (2)$$

$$\frac{1}{V} = \frac{1}{V_{\text{max}}} + \frac{K_m}{V_{\text{max}}} \frac{1}{[\text{S}]} \quad (3)$$

where V is the rate of *p*-NP formation, V_{max} is the maximum rate, K_{cat} is the catalytic rate constant, $[\text{E}_0]$ is the enzyme concentration, $[\text{S}]$ is the substrate concentration, K_m is the substrate concentration when the rate is equal to $V_{\text{max}}/2$, which also shows the affinity of the enzyme for the substrate, and K_{cat}/K_m is the kinetic constant that represents the enzyme's overall ability to convert the substrate to the product. The K_m and K_{cat}/K_m values for free BCA and composites are summarized in Table 2. The kinetic parameters K_m were found to be 8.92, 7.25, and 5.14 mM, and K_{cat}/K_m values were 399.80, 443.78, and 499.75 $\text{M}^{-1} \text{s}^{-1}$ for BCA, BCA/ZIF-8/CPVA, and BCA@ZIF-8/CPVA, respectively, indicating that both composites performed better than the free enzyme for the *p*-NPA hydrolysis. The low K_m means that the enzyme requires a lower substrate concentration to achieve V_{max} and usually suggests that the enzyme may have a higher affinity with the substrate. The value of K_m is sometimes equated with the dissociation constant of the enzyme–substrate complex, *ES*

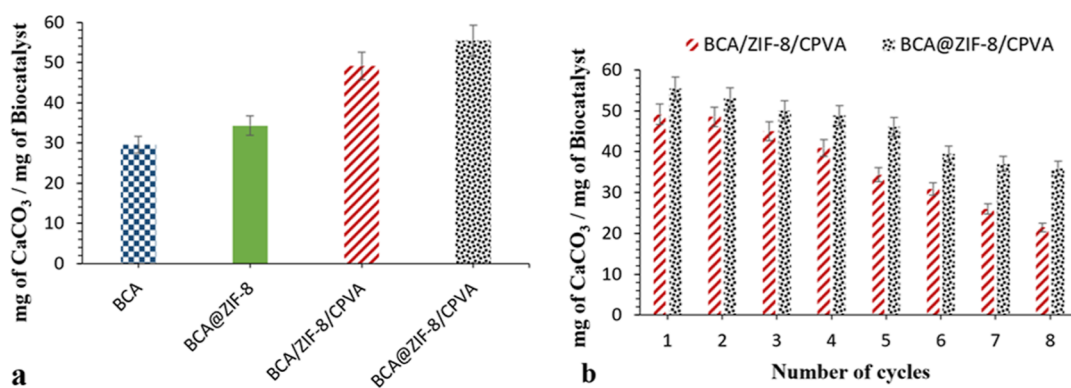


Figure 8. (a) Comparison of conversion of CO₂ to CaCO₃ by free and immobilized BAC, (b) recyclability of the biocatalysts [error bars are mean \pm standard deviation ($n = 3$)].

(the larger the K_m , the weaker the binding). In addition, the higher K_{cat}/K_m value for BCA@ZIF-8/CPVA may be due to the higher loading of BCA into this composite relative to the loading on BCA/ZIF-8/CPVA.

3.4. Effect of pH. As shown in Figure 7a, the effect of pH on the relative activity of both BCA/ZIF-8/CPVA and BCA@ZIF-8/CPVA was evaluated in the pH range of 6.0–10. The relative activity of the free and immobilized BCA showed a significant difference within this pH range. Furthermore, it is worth mentioning that the encapsulated BCA displayed a higher tolerance in the acidic regions compared to BCA/ZIF-8/CPVA and the free enzyme. Overall, it can be concluded that the encapsulation method seemed to result in enzyme tolerance enhancement in harsh conditions.

3.5. Thermal Stability. Being considered a critical point for industrial purposes, the thermal stability of the biocatalyst plays a pivotal role in the conformational transitions of the enzyme at high temperatures, which can result in a loss of catalytic activity. Consequently, the thermal stability of the biocatalyst could be improved *via* the immobilization of the enzyme into suitable carriers. Therefore, the relative activity of the free and immobilized BCA was investigated as a function of temperature in the range of 25 to 65 °C (Figure 7b). It is worth mentioning that the immobilized BCA performed better in all the evaluated temperatures (up to 65 °C) compared to its free counterpart, which refers to an improvement in stability.

Additionally, the BCA@ZIF-8/CPVA composite demonstrated a higher activity than the BCA/ZIF-8/CPVA composite. For instance, at 55 °C, the BCA@ZIF-8/CPVA and BCA/ZIF-8/CPVA composites were 50 and 35% more active than the free enzyme, respectively. The obtained results confirmed that encapsulating the BCA enzyme into MOFs could prevent its conformation transition at high temperatures and increase its thermal stability.

3.6. Storage Stability. Having permanent stability is crucial for nanocomposites in practical applications. In this manner, the storage stability of the free and immobilized enzymes in Tris buffer (50 mM, pH 8.0) was followed for 37 days at RT. As shown in Figure 7c, BCA@ZIF-8/CPVA and BCA/ZIF-8/CPVA are 63 and 43% more active than the free enzyme after 37 days, respectively. These results show MOF–polymer structure adequately protected the enzyme from denaturation and agglomeration that reduce enzyme activity during the storage time. However, encapsulated enzymes experienced better protection due to ZIF-8 acting as a shell and minimizing exposure to environmental parameters.

3.7. Reusability. The reusability of the enzyme, which is one of the main requirements for utilizing the biocatalysts to capture CO₂, is considered a fundamental factor for practical use. The results of eight cycles of hydrolysis of *p*-NPA by BCA@ZIF-8/CPVA and BCA/ZIF-8/CPVA are represented in Figure 7d. After each run, the prepared composite was separated and washed thoroughly with Tris buffer and immersed into the fresh substrate for the next run. The results demonstrated that the activity of the BCA@ZIF-8/CPVA composite reduced nearly 13% compared with its initial activity during almost eight cycles; however, this value for BCA/ZIF-8/CPVA was approximately 20%. The different performances of the biocomposites after eight cycles can be related to difference in the immobilization methods of BCA. As expected, the leaching possibility in the adsorption method is higher than in *in situ* encapsulation. The amount of BCA in the enzyme solution after the recycling test was determined using the Bradford method. The leaching of BCA enzyme was not detected for BCA@ZIF-8/CPVA, but the leaching amount for BCA/ZIF-8/CPVA was 17.6% of the initial loaded BCA. Therefore, the synthesized biocatalysts can be considered reusable sorbents for CO₂ capture and have the potential for industrial applications.

3.8. CO₂ Sequestration in CaCO₃. For CO₂ transformation, it is explicit that BCA@ZIF-8 was used to accelerate the mineralization of carbon dioxide to carbonates.³¹ To evaluate whether BCA/ZIF-8/CPVA and BCA@ZIF-8/CPVA could boost the CO₂ sequestration, we investigated the formation of CaCO₃ from CO₂ using BCA/ZIF-8/CPVA and BCA@ZIF-8/CPVA. The CO₂ sequestration capacity was quantized based on the conversion of CO₂ to CaCO₃. As expected, compared to free BCA and BCA@ZIF-8, the amount of calcium carbonate obtained using BCA/ZIF-8/CPVA and BCA@ZIF-8/CPVA is around 1.5-fold (Figure 8a). This result indicated that the presence of the CPVA fiber accelerated the recovery of BCA@ZIF-8 and improving reusability. Furthermore, the fibrous composites could be taken out directly from the reaction medium after the repeated catalytic reaction, while the BCA@ZIF-8 composite must be recovered from the reaction medium *via* centrifugation or filtration. Therefore, the BCA/ZIF-8/CPVA and BCA@ZIF-8/CPVA are more suitable for industrial applications than the BCA@ZIF-8 composite.

Figure 8b illustrates the eight cycles of CaCO₃ precipitation by biocomposites. As can be seen, the amount of the resulting CaCO₃ was still noticeable after eight cycles. Although in the case of BCA/ZIF-8/CPVA, the faster decrease in the yield of

CaCO₃ was observed due to the adsorption of BCA on the composite and subsequently more leaching compared to BCA@ZIF-8/CPVA. The decreased amount of calcium carbonate could be due to the denaturation of enzymes and the leaching under CO₂ bubbling, leading to increased internal pressure, and the reaction solution becomes acidic with CO₂ bubbling.^{27,49} However, BCA@ZIF-8/CPVA and BCA/ZIF-8/CPVA maintained 64.8 and 43.6% of their original activity after eight cycles, respectively. According to the XRD pattern and FT-IR spectra, the structure of the recovered biocatalyst was well maintained after the last cycle (Figures 1 and 2).

4. CONCLUSIONS

In conclusion, we immobilized BCA@ZIF-8 composites into the cross-linked PVA to attain BCA@ZIF-8/CPVA and BCA/ZIF-8/CPVA composites for improved CO₂ capture capacity. These biocatalysts displayed higher CO₂ transfer performance compared to the BCA@ZIF-8 composite. Furthermore, the prepared fibers can be recovered promptly from the reaction medium after the catalysis cycles without the need for high-speed centrifugation or filtration, which simplifies the separation process and decreases the production cost for industrial applications. Meanwhile, the BCA@ZIF-8/CPVA and BCA/ZIF-8/CPVA composites exhibited increased thermostability, acid resistance, and tolerance toward denaturants. The yields of the solid CaCO₃ obtained by using BCA@ZIF-8/CPVA and BCA/ZIF-8/CPVA were 55.45 and 49.15 mg, respectively, compared to 29.5 mg of CaCO₃ per mg of free BCA. Therefore, these excellent performances in harsh situations and effortless separation provided an excellent accelerator for CO₂ sequestration into CaCO₃, which can be useful in the industry. The outcomes indicated that the BCA@ZIF-8/CPVA and BCA/ZIF-8/CPVA composites are green, stable, reusable, and convenient biocatalysts for CO₂ sequestration catalytic applications under mild conditions.

■ ASSOCIATED CONTENT

SI Supporting Information

The Supporting Information is available free of charge at <https://pubs.acs.org/doi/10.1021/acsomega.3c00691>.

Preparation of electrospinning solutions; preparation of PVA fibers; Bradford assay of the protein concentration; BJH plots of ZIF-8/CPVA, BCA/ZIF-8/CPVA, and BCA@ZIF-8/CPVA composite; and DTG curves of ZIF-8/CPVA, BCA/ZIF-8/CPVA, and BCA@ZIF-8/CPVA composite (PDF)

■ AUTHOR INFORMATION

Corresponding Authors

Shahram Tangestaninejad – Department of Chemistry, Catalysis Division, University of Isfahan, Isfahan 81746-73441, Iran; orcid.org/0000-0001-5263-9795; Email: stanges@sci.ui.ac.ir

Majid Moghadam – Department of Chemistry, Catalysis Division, University of Isfahan, Isfahan 81746-73441, Iran; orcid.org/0000-0001-8984-1225; Email: moghadamm@sci.ui.ac.ir

Valiollah Mirkhani – Department of Chemistry, Catalysis Division, University of Isfahan, Isfahan 81746-73441, Iran; Email: mirkhani@sci.ui.ac.ir

Authors

Vahideh Asadi – Department of Chemistry, Catalysis Division, University of Isfahan, Isfahan 81746-73441, Iran;

orcid.org/0000-0002-2375-6500

Afsaneh Marandi – Department of Chemistry, Catalysis Division, University of Isfahan, Isfahan 81746-73441, Iran;

orcid.org/0000-0001-7599-7771

Reihaneh Kardanpour – Department of Chemistry, Catalysis Division, University of Isfahan, Isfahan 81746-73441, Iran

Iraj Mohammadpoor-Baltork – Department of Chemistry, Catalysis Division, University of Isfahan, Isfahan 81746-73441, Iran; orcid.org/0000-0001-7998-5401

Razieh Mirzaei – Department of Chemistry, Catalysis Division, University of Isfahan, Isfahan 81746-73441, Iran

Complete contact information is available at:

<https://pubs.acs.org/doi/10.1021/acsomega.3c00691>

Author Contributions

V.A.: material synthesis, characterization, data analysis, evaluation of catalytic activity, and writing the original draft. A.M. and R.K.: writing and editing the manuscript. S.T., M.M., and V.M.: conceptualization, methodology, supervision, and project administration. I.M.-B.: conceptualization.

Notes

The authors declare no competing financial interest.

■ ACKNOWLEDGMENTS

We are grateful to the Research Council of the University of Isfahan for the financial support of this work.

■ ABBREVIATIONS

BCA, bovine carbonic anhydrase; CA, carbonic anhydrase; CPVA, cross-linked electrospun polyvinyl alcohol; PVA, polyvinyl alcohol; MOF, metal–organic framework; ZIF-8, zeolitic imidazolate framework-8; TEA, trimethylamine; *p*-NP, *p*-nitrophenol; *p*-NPA, *p*-nitrophenyl acetate; GA, glutaraldehyde

■ REFERENCES

- (1) Li, J.-R.; Sculley, J.; Zhou, H.-C. Metal–organic frameworks for separations. *Chem. Rev.* **2012**, *112*, 869–932.
- (2) Yang, H.; Liu, J.; Jiang, K.; Meng, J.; Guan, D.; Xu, Y.; Tao, S. Multi-objective analysis of the co-mitigation of CO₂ and PM_{2.5} pollution by China's iron and steel industry. *J. Cleaner Prod.* **2018**, *185*, 331–341.
- (3) Hong, S.-G.; Jeon, H.; Kim, H. S.; Jun, S.-H.; Jin, E.; Kim, J. One-pot enzymatic conversion of carbon dioxide and utilization for improved microbial growth. *Environ. Sci. Technol.* **2015**, *49*, 4466–4472.
- (4) Gladis, A.; Gundersen, M. T.; Fosbøl, P. L.; Woodley, J. M.; von Solms, N. Influence of temperature and solvent concentration on the kinetics of the enzyme carbonic anhydrase in carbon capture technology. *Chem. Eng. J.* **2017**, *309*, 772–786.
- (5) Oviya, M.; Giri, S. S.; Sukumaran, V.; Natarajan, P. Immobilization of carbonic anhydrase enzyme purified from *Bacillus subtilis* VSG-4 and its application as CO₂ sequesterer. *Prep. Biochem. Biotechnol.* **2012**, *42*, 462–475.
- (6) Franssen, M. C.; Steunenberg, P.; Scott, E. L.; Zuilhof, H.; Sanders, J. P. Immobilised enzymes in biorenewables production. *Chem. Soc. Rev.* **2013**, *42*, 6491–6533.
- (7) Iliuta, I.; Iliuta, M. C. Investigation of CO₂ removal by immobilized carbonic anhydrase enzyme in a hollow-fiber membrane bioreactor. *AIChE J.* **2017**, *63*, 2996–3007.

- (8) Mohamad, N. R.; Marzuki, N. H. C.; Buang, N. A.; Huyop, F.; Wahab, R. A. An overview of technologies for immobilization of enzymes and surface analysis techniques for immobilized enzymes. *Biotechnol. Biotechnol. Equip.* **2015**, *29*, 205–220.
- (9) Park, J.-M.; Kim, M.; Lee, H. J.; Jang, A.; Min, J.; Kim, Y.-H. Enhancing the production of *Rhodobacter sphaeroides*-derived physiologically active substances using carbonic anhydrase-immobilized electrospun nanofibers. *Biomacromolecules* **2012**, *13*, 3780–3786.
- (10) Liu, S.; Bilal, M.; Rizwan, K.; Gul, I.; Rasheed, T.; Iqbal, H. M. Smart chemistry of enzyme immobilization using various support matrices—A review. *Int. J. Biol. Macromol.* **2021**, *190*, 396–408.
- (11) Patel, H.; Rawtani, D.; Agrawal, Y. A newly emerging trend of chitosan-based sensing platform for the organophosphate pesticide detection using Acetylcholinesterase—A review. *Trends Food Sci. Technol.* **2019**, *85*, 78–91.
- (12) Kumar, A.; Park, G. D.; Patel, S. K.; Kondaveeti, S.; Otari, S.; Anwar, M. Z.; Kalia, V. C.; Singh, Y.; Kim, S. C.; Cho, B.-K.; et al. SiO₂ microparticles with carbon nanotube-derived mesopores as an efficient support for enzyme immobilization. *Chem. Eng. J.* **2019**, *359*, 1252–1264.
- (13) Badoei-Dalfard, A.; Karami, Z.; Malekabadi, S. Construction of CLEAs-lipase on magnetic graphene oxide nanocomposite: an efficient nanobiocatalyst for biodiesel production. *Bioresour. Technol.* **2019**, *278*, 473–476.
- (14) Zhao, T.; Fan, Y.; Sun, Z.; Yang, J.; Zhu, X.; Jiang, W.; Wang, L.; Deng, Y.; Cheng, X.; Qiu, P.; et al. Confined interfacial micelle aggregating assembly of ordered macro-mesoporous tungsten oxides for H₂S sensing. *Nanoscale* **2020**, *12*, 20811–20819.
- (15) Zhao, T.; Qiu, P.; Fan, Y.; Yang, J.; Jiang, W.; Wang, L.; Deng, Y.; Luo, W. Hierarchical branched mesoporous TiO₂–SnO₂ nanocomposites with well-defined n–n heterojunctions for highly efficient ethanol sensing. *Adv. Sci.* **2019**, *6*, 1902008.
- (16) Feng, Y.; Xu, Y.; Liu, S.; Wu, D.; Su, Z.; Chen, G.; Liu, J.; Li, G. Recent advances in enzyme immobilization based on novel porous framework materials and its applications in biosensing. *Coord. Chem. Rev.* **2022**, *459*, 214414.
- (17) Qiu, Q.; Chen, H.; Wang, Y.; Ying, Y. Recent advances in the rational synthesis and sensing applications of metal-organic framework biocomposites. *Coord. Chem. Rev.* **2019**, *387*, 60–78.
- (18) Ren, S.; Chen, R.; Wu, Z.; Su, S.; Hou, J.; Yuan, Y. Enzymatic characteristics of immobilized carbonic anhydrase and its applications in CO₂ conversion. *Colloids Surf., B* **2021**, *204*, 111779.
- (19) Chen, G.; Kou, X.; Huang, S.; Tong, L.; Shen, Y.; Zhu, W.; Zhu, F.; Ouyang, G. Modulating the biofunctionality of metal-organic-framework-encapsulated enzymes through controllable embedding patterns. *Angew. Chem., Int. Ed.* **2020**, *59*, 2867–2874.
- (20) Jo, B. H.; Kim, I. G.; Seo, J. H.; Kang, D. G.; Cha, H. J. Engineered *Escherichia coli* with periplasmic carbonic anhydrase as a biocatalyst for CO₂ sequestration. *Appl. Environ. Microbiol.* **2013**, *79*, 6697–6705.
- (21) Alvizo, O.; Nguyen, L. J.; Savile, C. K.; Bresson, J. A.; Lakhapatri, S. L.; Solis, E. O.; Fox, R. J.; Broering, J. M.; Benoit, M. R.; Zimmerman, S. A.; et al. Directed evolution of an ultrastable carbonic anhydrase for highly efficient carbon capture from flue gas. *Proc. Natl. Acad. Sci. U.S.A.* **2014**, *111*, 16436–16441.
- (22) Arazawa, D.; Kimmel, J.; Finn, M.; Federspiel, W. Acidic sweep gas with carbonic anhydrase coated hollow fiber membranes synergistically accelerates CO₂ removal from blood. *Acta Biomater.* **2015**, *25*, 143–149.
- (23) Jo, B. H.; Seo, J. H.; Yang, Y. J.; Baek, K.; Choi, Y. S.; Pack, S. P.; Oh, S. H.; Cha, H. J. Bioinspired silica nanocomposite with autoencapsulated carbonic anhydrase as a robust biocatalyst for CO₂ sequestration. *ACS Catal.* **2014**, *4*, 4332–4340.
- (24) Prabhu, C.; Wanjari, S.; Gawande, S.; Das, S.; Labhsetwar, N.; Kotwal, S.; Puri, A. K.; Satyanarayana, T.; Rayalu, S. Immobilization of carbonic anhydrase enriched microorganism on biopolymer based materials. *J. Mol. Catal. B: Enzym.* **2009**, *60*, 13–21.
- (25) Bednár, A.; Nemestóthy, N.; Bakonyi, P.; Fülöp, L.; Zhen, G.; Lu, X.; Kobayashi, T.; Kumar, G.; Xu, K.; Bélafi-Bakó, K. Enzymatically-boosted ionic liquid gas separation membranes using carbonic anhydrase of biomass origin. *Chem. Eng. J.* **2016**, *303*, 621–626.
- (26) Ren, S.; Chen, R.; Wu, Z.; Su, S.; Hou, J.; Yuan, Y. Enzymatic characteristics of immobilized carbonic anhydrase and its applications in CO₂ conversion. *Colloids Surf., B* **2021**, *204*, 111779.
- (27) Cui, J.; Feng, Y.; Lin, T.; Tan, Z.; Zhong, C.; Jia, S. Mesoporous metal-organic framework with well-defined cruciate flower-like morphology for enzyme immobilization. *ACS Appl. Mater. Interfaces* **2017**, *9*, 10587–10594.
- (28) Zhang, S.; Du, M.; Shao, P.; Wang, L.; Ye, J.; Chen, J.; Chen, J. Carbonic anhydrase enzyme-MOFs composite with a superior catalytic performance to promote CO₂ absorption into tertiary amine solution. *Environ. Sci. Technol.* **2018**, *52*, 12708–12716.
- (29) Liu, Q.; Chapman, J.; Huang, A.; Williams, K. C.; Wagner, A.; Garapati, N.; Sierros, K. A.; Dinu, C. Z. User-tailored metal-organic frameworks as supports for carbonic anhydrase. *ACS Appl. Mater. Interfaces* **2018**, *10*, 41326–41337.
- (30) Ren, S.; Feng, Y.; Wen, H.; Li, C.; Sun, B.; Cui, J.; Jia, S. Immobilized carbonic anhydrase on mesoporous cruciate flower-like metal organic framework for promoting CO₂ sequestration. *Int. J. Biol. Macromol.* **2018**, *117*, 189–198.
- (31) Asadi, V.; Kardanpour, R.; Tangestaninejad, S.; Moghadam, M.; Mirkhani, V.; Mohammadpoor-Baltork, I. Novel bovine carbonic anhydrase encapsulated in a metal-organic framework: a new platform for biomimetic sequestration of CO₂. *RSC Adv.* **2019**, *9*, 28460–28469.
- (32) Cui, J.; Feng, Y.; Jia, S. Silica encapsulated catalase@metal-organic framework composite: A highly stable and recyclable biocatalyst. *Chem. Eng. J.* **2018**, *351*, 506–514.
- (33) Feng, Y.; Zhong, L.; Bilal, M.; Tan, Z.; Hou, Y.; Jia, S.; Cui, J. Enzymes@ZIF-8 nanocomposites with protection nanocoating: stability and acid-resistant evaluation. *Polymers* **2018**, *11*, 27.
- (34) Feng, Y.; Zhong, L.; Hou, Y.; Jia, S.; Cui, J. Acid-resistant enzyme@MOF nanocomposites with mesoporous silica shells for enzymatic applications in acidic environments. *J. Biotechnol.* **2019**, *306*, 54–61.
- (35) Bercea, M.; Bibire, E.-L.; Morariu, S.; Carja, G. Chitosan/poly(vinyl alcohol)/LDH biocomposites with pH-sensitive properties. *Int. J. Polym. Mater. Polym. Biomater.* **2015**, *64*, 628–636.
- (36) Wu, Y.-n.; Li, F.; Liu, H.; Zhu, W.; Teng, M.; Jiang, Y.; Li, W.; Xu, D.; He, D.; Hannam, P.; et al. Electrospun fibrous mats as skeletons to produce free-standing MOF membranes. *J. Mater. Chem.* **2012**, *22*, 16971–16978.
- (37) Lin, R.; Ge, L.; Diao, H.; Rudolph, V.; Zhu, Z. Ionic liquids as the MOFs/polymer interfacial binder for efficient membrane separation. *ACS Appl. Mater. Interfaces* **2016**, *8*, 32041–32049.
- (38) Hess, S. C.; Grass, R. N.; Stark, W. J. MOF channels within porous polymer film: flexible, self-supporting ZIF-8 poly(ether sulfone) composite membrane. *Chem. Mater.* **2016**, *28*, 7638–7644.
- (39) Ren, S.; Li, C.; Tan, Z.; Hou, Y.; Jia, S.; Cui, J. Carbonic Anhydrase@ZIF-8 Hydrogel Composite Membrane with Improved Recycling and Stability for Efficient CO₂ Capture. *J. Agric. Food Chem.* **2019**, *67*, 3372–3379.
- (40) Dai, X.; Cao, Y.; Shi, X.; Wang, X. The PLA/ZIF-8 nanocomposite membranes: the diameter and surface roughness adjustment by ZIF-8 nanoparticles, high wettability, improved mechanical property, and efficient oil/water separation. *Adv. Mater. Interfaces* **2016**, *3*, 1600725.
- (41) Liu, C.; Wu, Y.-n.; Morlay, C.; Gu, Y.; Gebremariam, B.; Yuan, X.; Li, F. General deposition of metal-organic frameworks on highly adaptive organic-inorganic hybrid electrospun fibrous substrates. *ACS Appl. Mater. Interfaces* **2016**, *8*, 2552–2561.
- (42) Puguang, J. M. C.; Kim, H.-S.; Lee, K.-J.; Kim, H. Low internal concentration polarization in forward osmosis membranes with hydrophilic crosslinked PVA nanofibers as porous support layer. *Desalination* **2014**, *336*, 24–31.
- (43) Mirzaei, R.; Bahadori, M.; Kardanpour, R.; Rafiei, S.; Tangestaninejad, S.; Moghadam, M.; Mirkhani, V.;

Mohammadpoor-Baltork, I.; Mirazimi, S. E. Preparation and characterization of nanofibrous metal–organic frameworks as efficient catalysts for synthesis of cyclic carbonates in the solvent free conditions. *Dalton Trans.* **2021**, *50*, 10567–10579.

(44) Bradford, M. M. A rapid and sensitive method for the quantitation of microgram quantities of protein utilizing the principle of protein-dye binding. *Anal. Biochem.* **1976**, *72*, 248–254.

(45) Hou, J.; Dong, G.; Xiao, B.; Malassigne, C.; Chen, V. Preparation of titania based biocatalytic nanoparticles and membranes for CO₂ conversion. *J. Mater. Chem. A* **2015**, *3*, 3332–3342.

(46) Park, K. S.; Ni, Z.; Côté, A. P.; Choi, J. Y.; Huang, R.; Uribe-Romo, F. J.; Chae, H. K.; O’Keeffe, M.; Yaghi, O. M. Exceptional chemical and thermal stability of zeolitic imidazolate frameworks. *Proc. Natl. Acad. Sci. U.S.A.* **2006**, *103*, 10186–10191.

(47) Hu, Y.; Kazemian, H.; Rohani, S.; Huang, Y.; Song, Y. In situ high pressure study of ZIF-8 by FTIR spectroscopy. *Chem. Commun.* **2011**, *47*, 12694–12696.

(48) Wang, Q.; Zhang, X.; Huang, L.; Zhang, Z.; Dong, S. GOx@ZIF-8 (NiPd) nanoflower: An artificial enzyme system for tandem catalysis. *Angew. Chem.* **2017**, *129*, 16298–16301.

(49) Ren, S.; Li, C.; Tan, Z.; Hou, Y.; Jia, S.; Cui, J. Carbonic anhydrase@ZIF-8 hydrogel composite membrane with improved recycling and stability for efficient CO₂ capture. *J. Agric. Food Chem.* **2019**, *67*, 3372–3379.

(50) Zhang, Y.; Wang, H.; Liu, J.; Hou, J.; Zhang, Y. Enzyme-embedded metal–organic framework membranes on polymeric substrates for efficient CO₂ capture. *J. Mater. Chem. A* **2017**, *5*, 19954–19962.

(51) Dai, Y.; Tang, Q.; Zhang, Z.; Yu, C.; Li, H.; Xu, L.; Zhang, S.; Zou, Z. Enhanced mechanical, thermal, and UV-shielding properties of poly(vinyl alcohol)/metal–organic framework nanocomposites. *RSC Adv.* **2018**, *8*, 38681–38688.